Low-Speed Impact Craters in Loose Granular Media

J. S. Uehara, M. A. Ambroso, R. P. Ojha, and D. J. Durian
UCLA Department of Physics & Astronomy, Los Angeles, California 90095-1547, USA
(Received 29 January 2003; published 13 May 2003)

We report on craters formed by balls dropped into dry, noncohesive, granular media. By explicit variation of ball density ρ_b, diameter D_b, and drop height H, the crater diameter is confirmed to scale as the $1/4$ power of the energy of the ball at impact: $D_c \sim (\rho_b D_b^3 H)^{1/4}$. Against expectation, a different scaling law is discovered for the crater depth: $d \sim (\rho_b^{3/2} D_b^2 H)^{1/3}$. The scaling with properties of the medium is also established. The crater depth has significance for granular mechanics in that it relates to the stopping force on the ball.

DOI: 10.1103/PhysRevLett.90.194301 PACS numbers: 45.70.Ht, 45.70.Cc, 83.80.Fg, 89.75.Da

Sand is fragile: If you set down a ball, no matter how gingerly or how roughly, the sand can barely support the ball's weight; one slight tap and the ball digs in deeper. At the same time, sand can be very strong: If you drop the ball from some height, the sand can stop it quickly, forming a shallow crater in the process; a higher drop height will lead to only a slightly deeper crater. Similarly intriguing combinations of toughness and fragility have led to tremendous recent research activity into the physics of granular media in general [1,2]. At the scale of grain-grain interactions, there are only a few possible forces. There can be normal forces perpendicular to the contact plane, there can be static and sliding friction parallel to the contact plane, and there can be inelastic collisions. Since granular packings are random, the normal forces are random too but can be correlated over long distances in so-called "force chains." Dissipation can be either through inelastic collisions or sliding friction. But which of these is responsible for taking up the energy of an impacting ball?

Geophysicists have long been interested in the craters formed by impact or explosion [3–5]. Since meteorites generally strike at non-normal angles but nevertheless produce circular craters, it is believed that impacts can be likened to explosions. Extensive data for buried explosives and high-speed (km/s) ballistics impact indicate that the crater diameter D_c often scales as a power of energy. For example, the exponent is $1/3$ when the energy is dissipated by plastic flow of the medium throughout a volume $\sim D_c^3$; it is $1/4$ when the energy goes into lifting a volume $\sim D_c^3$ by a distance $\sim D_c$ against the force of gravity. This "gravity-limited" regime was recently observed in low-speed laboratory impact experiments [6]. There, steel balls of various diameters D_b were dropped into sand from various heights H; the resulting crater diameters scaled as $D_c \sim (D_b^3 H)^{1/4}$. For high-speed impacts in loose sand, however, ballistics data support $D_c \sim \rho_b^{1/3} D_b^{5/6} H^{1/6}$ [5,7].

Here we focus on the *depth* of craters formed by projectile impact. By contrast, the diameter has traditionally been the primary observable. Prior literature assumes that depth is proportional to diameter, as in explaining the scaling with energy, but this has not been checked in laboratory experiments. There are few actual observations, but "simple craters" formed by meteorite impact are thought to be parabolic with a depth equal to $1/5$ of the diameter [4] ("complex craters" are larger and exhibit flat floors or central peaks). The crater depth is also a key physical quantity because it relates to the force exerted by the medium onto the projectile. Specifically, if a ball of mass m is dropped from rest and forms a crater of depth d, then the average stopping force satisfies

$$\langle F \rangle d = mgH. \tag{1}$$

Note that H is the total drop distance, equal to the sum of initial height above the medium plus the depth of the crater. This simple experiment therefore gives a direct signature of the dissipation mechanics. We find that the depth d can be much less than the drop height H; therefore, to a suprising extent, *the dissipation force can far exceed the ball weight.* We also find that crater depth and diameter scale differently with ball density, ball diameter, and total drop distance. This contradicts common assumption [3–5]. So while our observations could lead to new insight into fundamental granular forces, they may also help in understanding geophysical craters: perhaps as a simple model system for comparison/contrast, and perhaps as a warning that crater depth need not be proportional to diameter unless explicity demonstrated. Of course, the detailed analogy between our low-speed impact craters and high-speed geophysical craters may be limited due to differences in the transport and dissipation mechanisms and in the role of cohesion. Limited analogy may also be sought for impact on metals [8,9].

Our experimental procedures are as follows. First, either a 1 or 2 L beaker is filled half way with a granular medium (results are independent of beaker size). The container is then horizontally swirled and lightly tapped in order to level the surface without noticeable compaction. Next a ball is fixed in the jaws of a wrench mounted to a ringstand. The ball is released with zero translational and rotational speed directly above the center of the

beaker. It splashes into the granular medium and comes to rest with some of its lower portion buried and its top fully exposed. This produces a crater with a circular rim that extends above the original horizontal surface of the medium. As is standard, we define the crater diameter by the location of maximum rim height. But now, we also measure the crater depth. Useful definitions might include the depth above which the ball is exposed, or the depth below which grains are not disturbed. Rather, to make contact with Eq. (1) and the average stopping force on the ball, we define the crater depth as the distance of the bottom of the ball below the initial horizontal surface of the medium. This is determined to ± 0.5 mm by measuring the location of the top exposed surface of the ball. Before proceeding, two bounds on the measured quantities should be noted. First, it is not possible to measure the crater diameter if it is less than the ball diameter. But even if the diameter is less than this minimum, the depth is still easily measured. Second, a ball dropped from infinitesimally above the surface of the medium can still penetrate to a nonzero depth, more so for denser balls. This defines a minimum crater depth, and corresponds to a minimum in total drop distance H. Our dynamic range for H is 1–1000 mm at best, but is more typically a factor of 100.

In Fig. 1 we show crater size vs loss in ball energy, $E = mgH$, for a variety of balls dropped into dry, monodisperse, 0.2 mm diameter glass beads. When so plotted, the diameter data collapse onto a power-law curve, $D_c = (0.24\text{cm/erg}^{1/4})E^{1/4}$. The crater diameter scaling is thus $D_c \sim (\rho_b D_b^3 H)^{1/4}$. This agrees with the gravity-limited scaling observation of Ref. [6]. Our data also extend that work, both in dynamic range and in explicit variation of the ball density. However, the most striking feature of Fig. 1 is that the crater depth data do not show a similar collapse. Apparently, the crater depth does not scale with the ball energy. Furthermore, it appears to follow a different power law with total drop distance, $d \sim H^{1/3}$. The weighted average of the exponents for power-law fits vs H are 0.231 ± 0.005 for diameter and 0.318 ± 0.005 for depth; for individual data sets, the average uncertainty is 0.03. Against natural expectation and contrary to prior assumption [3–6], the crater depth and diameter are separate length scales set by different physics.

Before further analyzing the data in Fig. 1, two specific comparisons should be noted. First, the smaller nylon ball and the silicon rubber ball have nearly the same density and diameter, but have very different surface properties: nylon is slick and silicon rubber is tacky. But as seen in Fig. 1, the crater depth data for these two balls (◇ and +, respectively) are indistinguishable. Therefore, friction between the ball and grains cannot be the dissipation mechanism responsible for stopping the ball. Second, the "live" and "dead" balls have nearly the same density and diameter, but have very different restitution coefficients. But as seen in Fig. 1, the depth data for these two balls (● and ■, repectively) are indistinguishable.

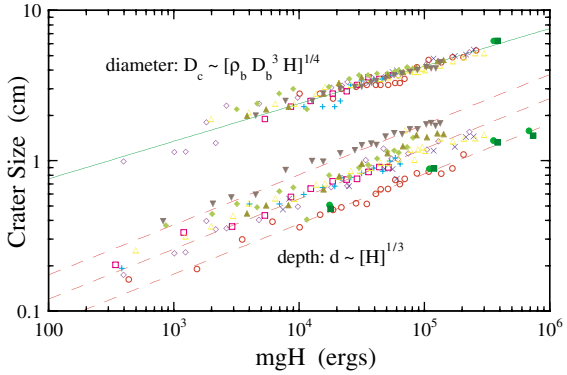

FIG. 1 (color online). The diameter and depth of craters formed by balls dropped into 0.2 mm diameter glass beads, as a function of total energy loss, $E = mgH$. Each data point represents the experimental result for a single drop height H. Plotting vs mgH collapses the diameter data, as seen earlier in Ref. [6], onto a 1/4 power law. By contrast, the depth data does not collapse, but follows a 1/3 power law. Symbol, ball type, ball density, and ball diameter are as follows: ○ for hollow plastic, 0.26 g/cm^3, 2.54 cm; □ for wood, 0.83 g/cm^3, 1.59 cm; ◇ for nylon, 1.10 g/cm^3, 1.59 cm; × for nylon, 1.10 g/cm^3, 2.54 cm; + for silicon rubber, 1.10 g/cm^3, 1.52 cm; △ for acrylic, 1.20 g/cm^3, 1.59 cm; ● for live ball, 1.20 g/cm^3, 3.82 cm; ■ for dead ball, 1.30 g/cm^3, 3.82 cm; ◆ for delrin, 1.40 g/cm^3, 1.59 cm; ▲ for Teflon, 2.20 g/cm^3, 1.59 cm; ▼ for ceramic, 3.90 g/cm^3, 1.27 cm. NB: Data for three even denser balls are omitted: stainless steel, 7.90 g/cm^3, 2.54 cm; lead, 11.3 g/cm^3, 1.13 cm; and tungsten carbide, 16.4 g/cm^3, 1.91 cm. These produce craters that also scale as $D_c \sim H^{1/4}$ and $d \sim H^{1/3}$; however, they do not exhibit the same $D_c \sim E^{1/4}$ collapse as the less dense balls.

Therefore, no significant energy is transferred to internal degrees of freedom of the ball.

We now explore the full form of the scaling laws for crater size. If the ball diameter and drop height are the only relevant length scales, then the simplest dimensionally correct laws consistent with the H dependence of Fig. 1 would be $D_c \propto D_b^{3/4} H^{1/4}$ and $d \propto D_b^{2/3} H^{1/3}$. To test this, we deduce the dimensionless proportionality constants for all the size vs H data. The results are plotted in Fig. 2(a) as a function of ball density. For the crater diameter, we find $D_c \sim \rho_b^{1/4}$ as expected from the above $E^{1/4}$ collapse. However, this trend is violated by the three densest balls (stainless steel, lead, and tungsten carbide), which were omitted from Fig. 1. For these three, the crater diameter is $D_c \approx 1.5 D_b^{3/4} H^{1/4}$ with no apparent dependence on ball density. For the crater depth, we have no *a priori* expectation other than that denser balls should penetrate deeper. The data in Fig. 2(a) are consistent with a simple power-law form, $d \sim \rho_b^{1/2}$; the uncertainty in the exponent is conservatively ± 0.05. Note that this holds for *all* balls, even the three densest where $D_c \sim \rho_b^{1/4}$ fails. As a final consistency check, the explicit dependence of crater size on ball diameter is shown in Fig. 2(b). Though the dynamic range is only a factor of 4,

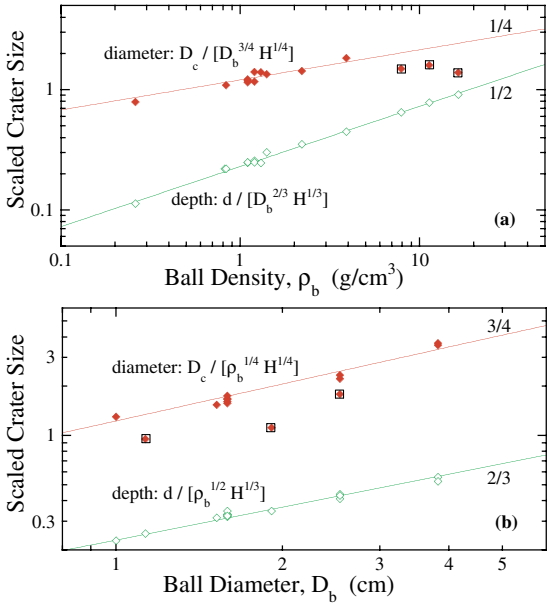

FIG. 2 (color online). Scaling of crater size with ball density and diameter. Each point represents the result of a $D_c \propto H^{1/4}$ or $d \propto H^{1/3}$ power-law fit to the size vs H data sets of Fig. 1, divided by the labeled combination of ball diameter or density and drop height; error bars are comparable to symbol size. All data are for 0.2 mm diameter glass beads. Note that the three densest balls do not obey the $D_c \sim \rho_b^{1/4}$ scaling; data for these balls are boxed in both (a) and (b).

the data are consistent with expectation, $D_c \sim D_b^{3/4}$ and $d \sim D_b^{2/3}$.

Next we vary the properties of the granular medium, studying craters formed by a 1-inch diameter nylon ball dropped into the media listed in Table I. Besides grain size, the other specifications are the (bulk) grain density ρ_g, and the angle of repose θ_r. Since identical cratering is found in 0.2 and 1 mm diameter glass beads, the grain size is not an important length scale (as suspected already based on the ball diameter and drop height scaling). Unless the ambient air plays a crucial role, the dependence on ρ_g must be the reciprocal of the dependence on ρ_b. We have no such guess for behavior vs θ_r. But since $\tan\theta_r$ is roughly the coefficient of friction between grains, it must play a role. To test all this we divide out the expected ρ_g dependence and plot the results vs $\tan\theta_r$ in Fig. 3. The dynamic range is only a factor of 2 for both ρ_g and $\mu = \tan\theta_r$, so power-law fits give exponents to within only ± 0.3. Nevertheless, the data are consistent with $D \sim (\rho_g \mu^2)^{-1/4}$ for the crater diameter and $d \sim (\rho_g \mu^2)^{-1/2}$ for the crater depth. Comfortingly, the same combination of material properties appears in both results, and also leads to a stopping force that is proportional to μ (next).

TABLE I. Specifications of the granular materials. The density refers to the bulk material, not the individual grains. The angle of repose, θ_r, was measured by the draining method [10], which seems most appropriate for craters; it gives the grain-grain friction coefficient as $\mu = \tan\theta_r$. The beach sand is the only significantly polydisperse material.

Material	Grain size (mm)	ρ_g (g/cm^3)	θ_r
Sprinkles	2×7	0.76	39°
Popcorn	$4 \times 6 \times 7$	0.87	34°
Rice	2×7	0.88	32°
Salt	0.5	1.30	38°
Glass beads	0.2 or 1.0	1.51	24°
Beach sand	0.5 ± 0.4	1.59	38°

The final crater diameter and depth laws established by Figs. 1–3 are, respectively,

$$D_c = 0.92[\rho_b/(\rho_g \mu^2)]^{1/4} D_b^{3/4} H^{1/4}, \quad (2)$$

$$d = 0.16[\rho_b/(\rho_g \mu^2)]^{1/2} D_b^{2/3} H^{1/3}. \quad (3)$$

Whereas the depth law holds for all our observations, the diameter law fails for dense balls, $\rho_b > 4$ g/cm^3 (at least for glass beads—the materials dependence of this breakdown has not been investigated). For a fixed granular material, the diameter data collapse onto a 1/4 power law when plotted vs $\rho_b D_b^3 H$ (as in Fig. 1); therefore, the diameter scales with ball energy at impact. By contrast, the depth data collapse onto a 1/3 power-law when plotted vs $\rho_b^{3/2} D_b^2 H$(not shown—but since the scatter for depth and diameter is the same in Figs. 2 and 3, the quality of collapse is also comparable); therefore, the depth scales as neither ball energy nor ball momentum at impact. The diameter and depth are separate lengths set by separate physics.

The crater depth d may be the more fundamental length scale, in that it naturally relates to the underlying granular mechanics. Energy conservation, Eq. (1), and the depth law, Eq. (3), give the *average* stopping force acting on the ball as

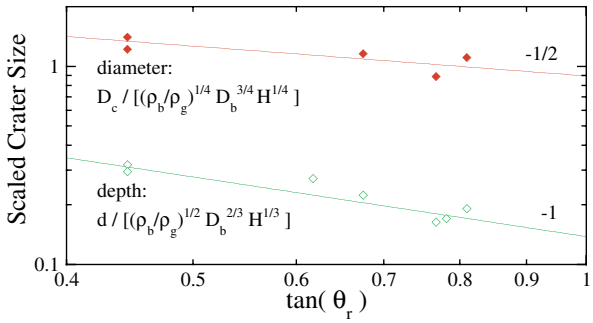

FIG. 3 (color online). Scaling of crater size with grain-grain friction coefficient, $\mu = \tan\theta_r$, for 1-inch diameter nylon ball dropped into the media specified in Table I. Each point represents the result of a $D_c \propto H^{1/4}$ or $d \propto H^{1/3}$ power-law fit to the size vs H data sets, divided by the labeled combination of ball and grain densities, ball diameter, and drop height; error bars are comparable to symbol size.

$$\frac{\langle F \rangle}{mg} = 6.3\mu\left(\frac{\rho_g}{\rho_b}\right)^{1/2}\left(\frac{H}{D_b}\right)^{2/3}. \quad (4)$$

Evidently, it can be much greater than the ball weight, mg, which the granular medium can barely support in a static situation. These results help constrain the form of the *instantaneous* stopping force on the ball throughout the impact process. If it varies only with ball speed, independent of depth, then it must scale as $F \sim v^{4/3}$. Alternatively, if the stopping force varies only with ball depth, independent of speed, then it must scale as $F \sim z^2$. Solution of $F = ma$ gives $d \sim H^{1/3}$ for both cases.

We now discuss these possible force laws in the context of the current understanding of granular mechanics. First, the kinetic theory of granular hydrodynamics gives a rate-dependent stopping force [11,12]. In Ref. [13] it was used to analyze the peak height of the granular jet formed when a heavy ball strikes the medium and becomes deeply submerged. There, the viscosity of the medium is proportional to the shear rate, which scales as ball speed divided by diameter. This gives a stopping force of $F \propto \rho_g D_g^2 v^2$, where D_g is the grain diameter and the numerical constant is set by the grain-grain restitution coefficient. This cannot account for our observations, since the dependencies on grain density, grain size, ball size, and ball speed are all wrong. Furthermore, a $F \sim v^2$ drag force is not even strong enough to bring an object to rest. A modification, whereby the viscosity increases with packing fraction [14], would be required.

Second, the lateral drag force on an object slowly pulled through a granular medium at constant depth is rate-independent, as in plowing a field. Recently it was found to scale as the product of the object's cross section and the hydrostatic pressure at that depth [15]. If this applies to our work, where the ball moves down rather than sideways, then the instantaneous drag force is proportional to the weight of displaced grains: $F = \eta\rho_g g\pi(D_b z^2/2 - z^3/3)$. Here z is the depth of the bottom of the ball, the volume of displaced grains equals the submerged volume of the ball, and η is a materials parameter like μ. For $z \ll D_b$, the leading term is $F \sim z^2$ and the final crater depth is $d = [(\rho_b/\rho_g)D_b^2 H/\eta]^{1/3}$. This is quite similar to our observation, Eq. (3); however the ball and grain density dependencies are incorrect. The parameter range in Fig. 2(a) is great enough to easily rule out $d \sim \rho_b^{1/3}$ in favor of $d \sim \rho_b^{1/2}$.

Altogether, it appears that our observation for the scaling of crater depth, Eq. (3), cannot be explained using prior work. Friction at the ball surface, collisional granular hydrodynamics, and the plowing of hydrostatic grains, are all ruled out. One possible scenario is that as the ball crashes into the medium, it jams together the grains underneath. The normal force between these grains thus becomes much greater than the hydrostatic pressure. As the ball moves, the grain contacts slide so that each dissipates a total amount of energy given by the normal force times grain size. New contacts are formed as the old ones break. This loading and breaking of force chains gives rise to the dissipation force that ultimately stops the ball. Another possibility is that dissipation is due to sliding friction between force chains and the surrounding unloaded grains. Further work is needed to model either effect. Perhaps the scaling of crater diameter, Eq. (2), could then be explained as a consequence of the stopping force between ball and grains.

We thank R. P. Behringer, S. R. Nagel, and J. A. Rudnick for helpful suggestions. This material is based upon work supported by the National Science Foundation under Grant No. 0070329.

Note added in proof.—A similar experiment has been reported, in which a steel ball was dropped into glass beads of varying size [16]. Since the impact energy was greater, and the granular packing may have been looser, the ball always became submerged. The crater diameter scaled as $H^{1/4}$; the crater depth (measured to the bottom of the crater, not the bottom of the ball) was about $1/8$ the diameter but increased with H. Striking similarities were seen in laboratory and planetary crater morphologies, and in their changes with impact energy.

[1] H. M. Jaeger, S. R. Nagel, and R. P. Behringer, Rev. Mod. Phys. **68**, 1259 (1996).
[2] J. Duran, *Sands, Powders, and Grains: An Introduction to the Physics of Granular Materials* (Springer, New York, 2000).
[3] *Impact and Explosion Cratering*, edited by D. J. Roddy, R. O. Pepin, and R. B. Merril (Pergamon Press, New York, 1978).
[4] H. J. Melosh, *Impact Cratering: A Geologic Process* (Oxford University Press, New York, 1989).
[5] K. Holsapple, Annu. Rev. Earth Planet. Sci. **21**, 333 (1993).
[6] J. Amato and R. Williams, Am. J. Phys. **66**, 141 (1998).
[7] H. J. Melosh and R. A. Beyer, computer code CRATER, University of Arizona, Tuscon, Arizona, 1999 (available at http://www.lpl.arizona.edu/tekton/crater.html).
[8] M. E. van Valkenburg, W. G. Clay, and J. H. Huth, J. Appl. Phys. **27**, 1123 (1956).
[9] *High Velocity Impact Dynamics*, edited by J. A. Zukas (Wiley, New York, 1990).
[10] R. L. Brown and J. C. Richards, *Principles of Powder Mechanics* (Pergamon Press, Oxford, 1970).
[11] R. Bagnold, Proc. R. Soc. London A **225**, 49 (1954).
[12] S. Savage and M. Sayed, J. Fluid Mech. **142**, 391 (1984).
[13] S. Thoroddsen and A. Shen, Phys. Fluids **13**, 4 (2001).
[14] L. Bocquet, W. Losert, D. Schalk, T. C. Lubensky, and J. P. Gollub, Phys. Rev. E **65**, 011307 (2002).
[15] I. Albert, J. G. Sample, A. J. Morss, S. Rajagopalan, A. L. Barabasi, and P. Schiffer, Phys. Rev. E **64**, 061303 (2001), and references therein.
[16] A. M. Walsh, K. E. Holloway, P. Habdas, and J. R. de Bruyn (to be published).